Trochlear surface reconstruction and evaluation based on laser scanner acquisition

Stefka Gueorguieva, Remi Synave, Christine Couture

Trochlear surface reconstruction and evaluation based on laser scanner acquisition

Gueorguieva,S. and Synave,R.
UMR 5800,
Laboratoire Bordelais de Recherche en Informatique
Université Bordeaux 1, France
{stefka,synave}@labri.fr

Couture-Veschambre,Ch.
UMR 5199 PACEA,
Laboratoire d'Anthropologie des Populations du Passé
Université Bordeaux 1, France
{c.couture}@anthropologie.u-bordeaux1.fr

***Abstract*—The purpose of this study is to investigate the accuracy, reproducibility and validation of linear measurements on digital reconstruction of the trochlear articular surface. Surface reconstruction is produced by a laser scanner acquisition pipeline that preserves rough data. Arc and chord measurements between chosen landmarks on physical specimens are simulated by geodesic path length evaluation on the corresponding digital models. The osteological specimens are issued from an archaeological series emerging from the "Soeurs Grises"'s cemetery (medieval sample, XV-XVIII century) located in Beauvais (Oise, France).**

I. 3D IMAGING IN DIGITAL ANTHROPOLOGY RESEARCH

Medical imaging application in digital anthropology is an area of growing researches [1], [2], [3], [4], [5], [6], [7], [8]. High resolution 3D digital representations enable accurate reconstruction and geometric morphometrics analysis of specimens. Computed tomography is presently acknowledged as one of the most important technique in digital anthropology. In particular, the reconstruction and the restoration of human fossil is widely viewed as a tool for cultural heritage preservation [4], [9]. Often, virtual reconstruction stands for the visualization of complex inner anatomical structures as cortical bone thickness [10], inner ear and endocranial volumes [2], [11]. Further, rapid prototyping produces 3D solid reproductions of the anatomical models [12], [13], [14], [15], [16]. The acquisition, reconstruction and reproduction are well-established as qualitative techniques. Less is done in evaluating of their potential as "quantitative tool". A great number of researches [17], [18], [19], [20], [21], [22], [10] illustrates the complexity of the measurement definition with respect to its precision, repeatability and validation. As for example, Spoor's work [10] assesses linear measurements of cortical bone thickness by computed tomography. The cortical bone CT scan measurements are compared with the measurements on the corresponding cortical bone physical sections in order to validate the range values. The reported maximum error range is of $\pm 0.1mm$ and fit to the "best possible accuracy" depending on the CT characteristics and reconstruction settings in use (slice thickness of $1.5mm$, spatial resolution is within the interval $[0.5mm, 0.6mm]$, and pixel size within $[0.16mm, 0.22mm]$ (see also [23]). Moreover, CT based measurements are performed in the same slice image. Localization of the cranial landmarks using CT scans is studied by [21]. A "gold standard" set of data, recording the relative positions of 35 landmarks on a collection of ten skulls, is used to evaluate the precision of the landmark locations. Measurements are carried out inside a single CT scan as well as inside two CT scan images. While the average difference in landmark locations within an CT scan is less than $0.5mm$ for the entire gold standard set, some distance measures within two CT scans have range error greater than $2.5mm$. An error distortion along the coordinate axes is also emphasized. Disparity between errors along the axes is an important drawback since it could invalidate the identification of outlines defined on the basis of particular space orientation. Further, using "fuzzy landmarks" [24], the average error could be reduced to $1.15mm$. More recently, a comparison between mandibular landmarks position computations from CT scans and by a 3D space digitizer [25] establishes a standard deviation in landmark coordinates of $1.136mm$ with respect to linear distance range within the limits of $[0.001mm, 3.889mm]$. The reported and discussed above distance measurements are linear distances. Neither curvilinear arc distance measurements nor surface area measurements are experimented as long as we know. Several authors conclude that in place of slice images, 3D reconstructions could result in error reduction. No matter of the support in use, physic specimen, numerical representation or synthetic reproduction, a geometric morphometrics based analysis requires precise localization of landmarks and measurements of not only of linear distances, but also of surface area and volume data features and regions of interest.

In the present work, rough data acquisition is based on the the laser scanner acquisition pipeline. Our goal is to demonstrate that laser scan based 3D reconstruction have good capacity for quantitative assessment of linear and curvilinear distances. Moreover, the mesh models that are a direct output of the acquisition pipeline can support iD, $0 \leq i \leq 3$, axis orientation independent linear and curvilinear measures within comparable precision and repeatability. All measures are validated in comparison with anthropometric measures taken with caliper and millimeter ruler band on the specimens.

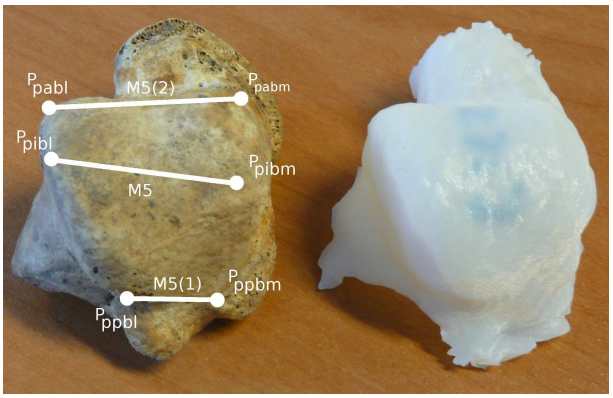

Fig. 1. Dorsal view of the trochlear surface of BCT92-S319-G and landmark point locations : (left) original specimen - (right) synthetic reproduction.

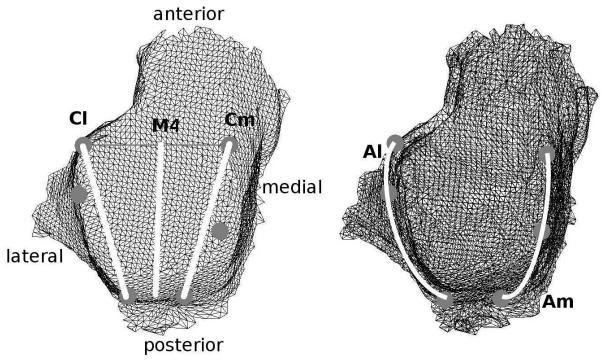

Fig. 2. Dorsal view of the trochlear surface of BCT92-S319-G and landmark point locations : (left) laser scanner acquisition - (right) solid mesh model.

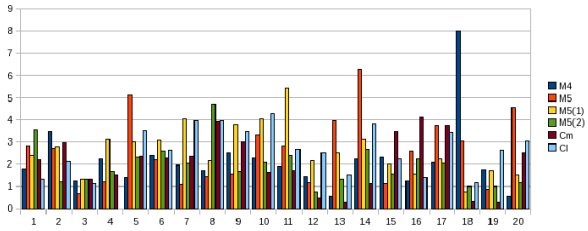

Fig. 3. STD of chord manual measurements on the series of 20 specimens.

II. Material and Methods

Landmark data from archaeological series

The studied *tali* are issued from an archaeological series emerging from the "Soeurs Grises"'s cemetery (medieval sample, XV-XVIII century) located in Beauvais (Oise, France). An almost exhaustive excavation was realized in 1992 and allowed the bring up to day of 350 inhumations and of about fifty ossuaries and reduced body individuals. Up to day, the specimen sample is composed of 350 adult specimens.

In the current study our interest is centered on a particular concavo-convex (trochlear) articular facet on the superior surface of the talus's body. In almost all specimens (10 pairs of left and right tali) the trochlea is relatively well preserved. It is strongly convex in the anterior direction, moderately concave in the mediolateral plane and wider distally than proximally.

Anatomically, the trochlea is very important articular facet since it is involved in the ankle joint and consequently in the foot position during locomotion [26]. The definitions and the locations of the landmark points follow [27], [28], [29]. Three pairs of landmark points for the trochlear shape are defined: $(P_{apmr}, P_{aplr}), (P_{ipmr}, P_{iplr})$ and (P_{ppmr}, P_{pplr}). Each pair corresponds to one position: the anterior, the intermediate and the posterior with respect to the frontal plan. A point of the pair is either on the medial or on the lateral process of the trochlea with respect to the sagittal plane, denoted as medial or lateral ridge. Landmark point location for the specimen $BCT92 - S319 - G$ are given in Fig. 1.

The anthropometric arc measures are with Mitutoyo digital caliper resolution of $0.01mm$. The chord measures are taken with a DKSH millimeter ruler band with expected accuracy of $1mm$. All the measurements quoted with "M" have been defined by Martin and Saller (1957) [27] and the others are new measurements introduced for the present study.

Let us define the anterior trochlea ridge as the curve starting in P_{apmr} passing through the anterior extremity of the medial lengthwise curvature of the trochlea and finishing in P_{aplr}. By analogy, the posterior trochlea ridge is defined between P_{ppmr} and P_{pplr}. The following landmark point distances are evaluated:

- $M4$ is the length of the chord joining the crossing points of the anterior and the posterior ridges with the medial lengthwise curvature of the trochlea.
-$M5$ is the length of the chord $P_{ipmr}P_{iplr}$;
-$M5(1)$ is the length of the chord $P_{ppmr}P_{pplr}$;
-$M5(2)$ is the length of the chord $P_{apmr}P_{aplr}$;
-Cm is the chord length $P_{ppmr}P_{apmr}$;
-Cl is the chord length $P_{pplr}P_{aplr}$;
-Am is the length of the arc joining P_{ppmr} and P_{apmr} along the medial ridge;
-Al is the length of the arc joining P_{pplr} and P_{aplr} along the lateral ridge.

The illustration is given in Fig. 1 and Fig. 2.

The error standard deviations (STD) of manual linear measurements on the series of 20 specimens are shown in Fig.3. As it is seen only 10.83% of the total number of chord measures have STD values under $1mm$, 40.83% are under $2mm$, and

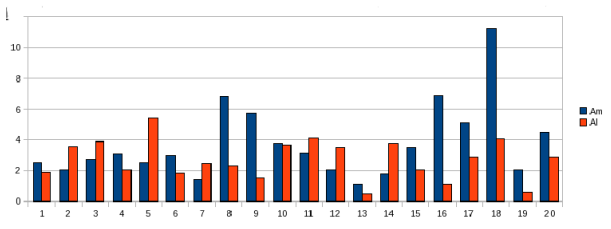

Fig. 4. STD of arc manual measurements on the series of 20 specimens.

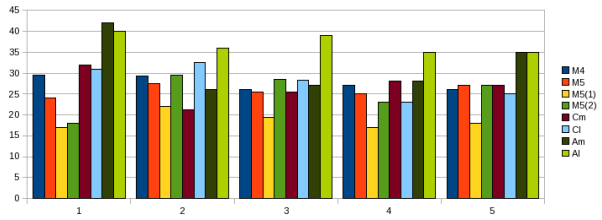

Fig. 5. Chord and arc manual measures of the specimen BCT92-S319-G.

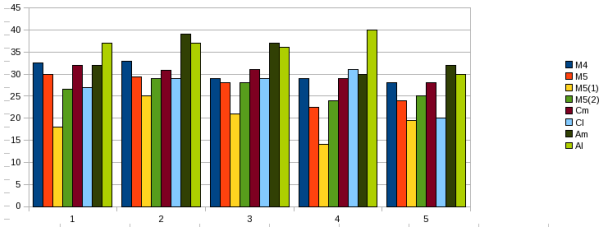

Fig. 6. Chord and arc manual measures of the specimen BCT92-S380-G.

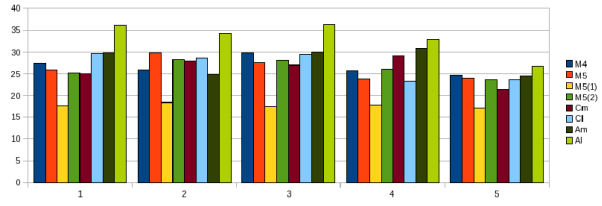

Fig. 7. Chord and arc numerical measures on 3D reconstruction of the specimen BCT92-S319-G.

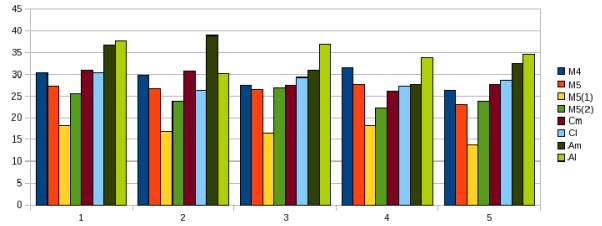

Fig. 8. Chord and arc numerical measures on 3D reconstruction of the specimen BCT92-S380-G.

74.17% are under $3mm$.

In the pursuit of the current knowledge, measures on two individuals, $BCT92-S319-G$ and $BCT92-S380-G$, will be expressly stated but issues for the rest of the studies talus collection are within the same limits. Range values for manual measures on the specimens $BCT92-S319-G$ and $BCT92-S380-G$ are given in Fig. 5 and Fig. 6.

The STD of manual arc measurements on the series of 20 specimens are shown in Fig.4. It could be seen that the curvilinear manual measures have bad performance: 5% of the total number of arc measures have STD values under $1mm$, 22.5% are under $2mm$, and 55% are under $3mm$.

LANDMARK DATA FROM IMAGE PROCESSING

The experimental platform in use consists of a 3D digitizer VIVID 300/VI-300, a software package A2RI and a printing system EDEN250.

The acquisition is done by a non-contact 3D digitizer VIVID 300/VI-300 with a laser wavelength $\lambda = 690nm$ and maximal optical power $P\_Max = 7mW$, object distance range in the limits of $[0.55m, 1.2m]$, field of view in the limits of $[185mm, 395mm]$ and output data points 400×400. In order to optimize the quality of the laser scans an acquisition protocol for the specimen acquisition is established [30] in such a way that laser power is fixed to 15% of P_Max, object distance is $550mm$, and the elongated triangles with aspect ratio superior to 4 of the scan borders are eliminated. During the acquisition, each specimen is exposed to the laser scan on a rotating stage set. The rotating stage is turned over the Z axis by a step of $45deg$ and thus producing 8 scans exported as triangular mesh models.

The software toolkit that supports the pipeline from the acquisition to the 3D printing is the $A2RI$[1] [31]. For each specimen, the input of $A2RI$ is the set of 8 triangular mesh models, one for each laser scan. The output is a 3D solid model of the specimen that could be exported in STL format for the printing by the 3D printing system. It should be emphasized that all treatments during the $A2RI$ processing do not approximate rough data. Thus all output mesh vertices correspond to acquired points on the specimen. In phantom studies [30] it has been shown that the precision of $A2RI$ is within the limits of $[0.72mm, 1.2mm]$ for linear distances and of $[0.68mm, 1.46mm]$ for curvilinear geodesic distances.

Finally, the 3D printing system Eden250 used for the specimen reproduction has a "typical" accuracy in the limits of $[0.1mm, 0.2mm]$[2]. The synthetic reproduction of $BCT92-S319-G$ processed by our pipeline is given in Fig. 1 (right).

Chord measures on the numerical representations of the specimen are calculated as Euclidean distances between the vertices corresponding to the landmark points (cf Fig. 2 (left)). Arc measures fit to the length of the geodesic paths that join these vertices and that follow the surface ridges (cf Fig. 2 (right)). Range values for numerical measures on the 3D reconstructions of the specimens $BCT92-S319-G$ and $BCT92-S380-G$ are given in Fig. 7 and Fig. 8.

The STD of the measures on the 3D reconstructions of $BCT92-S319-G$ and $BCT92-S380-G$ are given in Fig. 9 and Fig. 10. For chord measures on the $BCT92-S319-G$ reconstruction, $56,67\%$ are under $1mm$, $86,67\%$ are under $2mm$ and $96,67\%$ are under $3mm$. For the $BCT92-S380-G$ reconstruction, $56,67\%$ are under $1mm$, 83.33% are under $2mm$ and 100% are under $3mm$. With respect to arc measures on the $BCT92-S319-G$ representation, 30% are under $1mm$, 70% are under $2mm$ and 90% are under $3mm$. For the

[1] $A2RI$ could be download at $http://liba2ri.free.fr$

[2] According to the technical specifications and depending on the geometry, part orientation and print size.

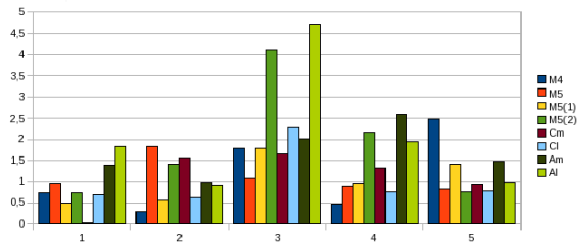

Fig. 9. STD of chord and arc measures on the 3D reconstruction of BCT92-S319-G.

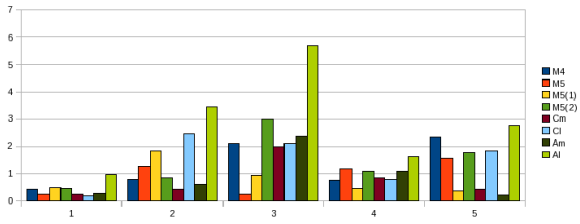

Fig. 10. STD of chord and arc measures on the 3D reconstruction of BCT92-S380-G.

$BCT92-S380-G$ model, 40% are under $1mm$, 60% are under $2mm$ and 80% are under $3mm$.

III. Results

Concerning the error of the linear distance measures on 3D reconstructions and for a total of 128 measures, STD are within the interval $[0.19mm, 2.98mm]$ for the model of $BCT92-S319-G$ and within the limits $[0.01mm, 4.12mm]$ for the model of $BCT92-S380-G$.
The anterior width $M5(2)$ of $BCT92-S380-G$ joining the medial and the lateral ridges respectively in P_{apmr} and P_{aplr} presents a damaged neighborhood around P_{apmr} that mislead the laser scanner acquisition and reconstruction in this region. The range intervals are comparable to the ones for the landmark point coordinate calculation given by [21] and [24] and obtained from CT slide images.

With respect to the reproducibility, numerical measures are more stable as long as in all experiments the population of numerical measures with STD under given threshold is greater than the one for manual measures. For example, 80% of numerical measures have STD under $2mm$ while for the manual measures only $36,6\%$ achieve this precision.

The validity of the numerical measures is tested in comparison with the manual measures. Table I recapitulates results for both $BCT92-S319-G$ and $BCT92-S380-G$ specimens. A visual feedback of the $3D$ models and measures used in the table is given in Fig. 12.

The absolute differences between numerical and manual measure values are given in the 4rd and the 7th columns. It can be seen that all absolute differences for linear distances are under $2mm$ except for $M5(1)$ on $BCT92-S380-G$. In Fig. 13 from the medial and posterior view of $BCT92-S380-G$ it

Fig. 11. BCT92-S319-G: (left) Medial view - (right) Lateral view

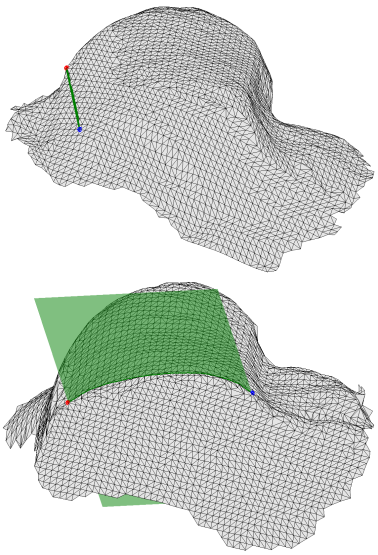

Fig. 12. Numerical models and measures of specimens $BCT92-S319-G$ and $BCT92-S380-G$: (up) M5(1), chord measure on $BCT92-S319-G$ - (bottom) Cl, arc measure on $BCT92-S380-G$

could be noticed that the osteological surface around P_{ppmr} is damaged that mislead landmark point location.

Arc measures for $BCT92-S380-G$ are less precise. Indeed, as it seen from the medial and lateral profiles in Fig.11, ridge extremities are damaged that make difficult the landmark point location.

IV. Discussion and conclusion

From an anatomical point of view one can conclude that the posterior width $M5(1)$ is stable all over the processing and could be retained as representative trochlear surface shape

Fig. 13. BCT92-S380-G: (left) Medial view - (right) Posterior view

	S319-G Numerical	S319-G Manual	S319-G Abs. diff.	S380-G Numerical	S380-G Manual	S380-G Abs. diff.
M4	26,77	27,56	0,79	28,96	30,3	1,34
M5	25,75	25,8	0,05	26,14	26,76	0,62
M5(1)	17,62	18,72	1,1	16,57	19,5	2,93
M5(2)	26,13	25,2	0,93	24,49	26,5	2,01
Cm	26,02	26,74	0,72	28,1	30,18	2,08
Cl	26,36	27,96	1,6	28,45	27,2	1,25
Am	28,21	31,6	3,39	32,32	34	1,68
Al	32,78	37	4,22	34,9	36	1,11

TABLE I
VALIDATION OF NUMERICAL MEASURES FOR SPECIMENS BCT92-S319-G AND BCT92-S380-G.

feature. Further, measures on the medial trochlea ridges are less exact. The chord measures are always better than the arc ones. This implies that the representative points location is quite precise but the distances measured along trochlea ridges necessitate more accurate computation. That is important because arc distances and curvature along medial and lateral trochlea ridges are related to functional anatomy of the human foot.

For the time being, our interest is directed to shape surface estimation in regions with constraint curvature variation corresponding to contact area of the talus articular surface.

Our believe is that $3D$ laser scanner based image acquisition and reconstruction are well-fitted to a precise quantitative estimation of surface shape features as linear and curvilinear distances, curvature and surface area appreciation.

ACKNOWLEDGMENT

The authors wish to thank Mr. P. Courtaud (UMR PACEA, LAPP) for providing the collection from Pessac osteological repository, and Mr. J.-M. Femolan in charge of the complete collection from Archaeological Department of Beauvais city concil.

REFERENCES

[1] L. Aiello, B. Wood, C. Key, and C. Wood, "Laser scanning and paleoanthropology: an example from olduvai gorge,tanzania," in *Primate Locomotion:Recent Advances*, 1998.

[2] C. Zollikofer, M. Ponce de Leon, and R. Martin, "Computer-assisted paleoanthropology," *Evolutionary Anthropology*, vol. 6, pp. 41–54, 1998.

[3] W. Recheis, G. Weber, K. Schaefer, R. Knapp, H. Seidler, and D. Nedden, "New methods and techniques in anthropology," in *Coll. Antropology*, vol. 23, 1999, pp. 495–509.

[4] F. Spoor, N. Jeffery, and F. Zonneveld, "Using diagnostic radiology in human evolutionary studies," *Journal of Anatomy*, vol. 197, pp. 61–76, 2000.

[5] G. Subsol, B. Mafart, M. De Lumley, and A. Silvestre, "3d image processing for the study of the evolution of the shape of the human skull: presentation of the tools and preliminary results." in *3D imaging in paleoanthropology and prehistoric archaeology*, 2001, pp. 1–10.

[6] G. Weber, "Virtual anthropology (va): a call for glastnost in paleoanthropology," *The Anatomical Record*, vol. 265, pp. 193–201, 2001.

[7] F. Zonneveld, "Applications and pitfalls of ct-based 3d imaging of hominid fossils," in *3D Imaging in Paleoanthropology and Prehistoric Archaeology*, 2001, pp. 5–9.

[8] B. Mafart, G. Guipert, M. Lumley, and G. Subsol, "Three-dimensional computer imaging of hominid fossils: a new step in human evolution studies," *Journal of Americal College of Radiology*, vol. 55, no. october, pp. 264–270, 2004.

[9] E. Bruner and G. Manzi, "Digital tools for the preservation of human fossil heritage: Ceprano, saccopastore, and other case studies," *Human Evolution*, vol. 21, pp. 33–44, 2006.

[10] C. Spoor, F. Zonneveld, and G. Macho, "Linear measurements of cortical bone and dental enamel by computed tomography: applications and problems," *American Journal of Physical Anthropology*, vol. 91, pp. 469–484, 1993.

[11] N. Ayache, "Epidaure: A research project in medical image analysis, simulation and robotics at inria," *IEEE Trans. Med. Imaging*, vol. 22, no. 10, pp. 1185–1201, 2003.

[12] N. Mankovich, A. Cheeseman, and N. Stoker, "The display of three-dimensional anatomy with stereolithographic models," *Journal of digital imaging*, vol. 3, no. 3, pp. 200–203, 1990.

[13] H. Seidler, D. Falk, C. Stringer, H. Wilfing, G. Muller, D. Nedden, G. Weber, W. Reicheis, and J. Arsuaga, "A comparative study of stereolithographically modelled skulls of petralona and broken hilll: implications for future studies of middle pleistocene hominid evolution," *Human Evolution*, vol. 33, pp. 691–703, 1997.

[14] Flaczynski.M., S. Corbel, and R. Jacquet, "Modélisation informatique et stéréolithographique d'un crâne sec nubien daté de 2700 ans et présentant une cranioténose," in *10ème Assises Européennes de prototypage rapide*, 2004, pp. 1–12.

[15] D. Zelicourt, K. Pekkan, H. Kitajima, D. Frakes, and A. Yoganathan, "Single-step stereolothography of complex anatomical models for optical flow measurements," *Transactions of the ASME*, vol. 127, pp. 204–207, february 2005.

[16] T. Allard, M. Sitchon, R. Sawatzky, and R. Hoppa, "Use of hand-held laser scanning and 3d printing for creation of a museum exhibit," in *6th International Symposium on Virtual Reality, Archaelogy and Cultural Heritage*, 2005.

[17] W. Jungers and R. Minns, "Computed tomography and biomechanical analysis of fossil long bones," *American journal of physical anthropology*, vol. 50, pp. 285–290, 1979.

[18] J. Tate and C. Cann, "High-resolution computed tomography for the comparative study of fossil and extant bone," *American Journal of Physical Anthropology*, vol. 58, pp. 67–73, 1982.

[19] D. Sumner, B. Mockbee, K. Morse, T. Cram, and M. Pitt, "Computed tomography and automated image analysis of prehistoric femora," *American Journal of Physical Anthropology*, vol. 68, pp. 225–232, 1985.

[20] C. Ruff and F. Leo, "Use of computed tomography in skeletal structure research," *Yearbook of physical anthropology*, vol. 29, pp. 181–196, 1986.

[21] J. Richtsmeier, C. Paik, P. Elfert, T. Cole, and H. Dahlman, "Precision, repeatability, and validation of the localization of cranial landmarks using computed tomography scans," *Cleft Palate-Craniofacial Journal*, vol. 32, no. 3, pp. 217–227, May 1995.

[22] C. Hildebolt, M. Vannier, and R. Knapp, "Validation study of skull three-dimensional computerized tomography measurements," *American journal of physical anthropology*, vol. 82, pp. 283–294, 1990.

[23] F. Zonneveld, "The technique of direct multiplanar high resolution ct of the temporal bone," *Neurosurgical Review*, vol. 8, pp. 5–13, 1985.

[24] C. Valeri, T. Cole, S. Lele, and J. Richtsmeier, "Capturing data from three dimensiona surfaces using fuzzy landmarks," *American Journal of Physical Anthropology*, vol. 107, pp. 113–124, 1998.

[25] F. Williams and J. Richtsmeier, "Comparaison of mandibular landmarks from computed tomography and 3d digitizer," *Clinical Anatomy*, vol. 16, pp. 494–500, 2003.

[26] B. Wood, L. Aiello, C. Wood, and C. Key, "A technique for establishing the identity of "isolated" fossil hominin limb bones," *Journal of Anatomy*, vol. 193, pp. 61–72, 1998.

[27] M. R. and K. Saller, *Lehrbuch der Anthropologie*. Bd 1 Fischer G Verlag, Stuttgart, 1957.

[28] L. Scheuer and S. Black, *The development of juvenile osteology*. Academic Press, 2000.

[29] B. De la Villetanet, "Utilisation d'outils de mesures en 3d dans le cadre d'une etude comparative morphofonctionnelle de tali d'hominoides actuel et du hominide fossile," Univ. Bordeaux I, MS,spécialité anthropologie, Tech. Rep. Octobre, 2005.

[30] R. Synave, "Reconstruction de solides à partir d'acquisitions surfaciques," Ph.D. dissertation, Université de Bordeaux1, 2009.

[31] R. Synave, P. Desbarats, and S. Gueorguieva, "Toolkit for registration and evaluation for 3d laser scanner acquisition," in *WSCG'2008, Proc. of the 16th International Conference in Central Europe on Computer Graphics, Visualisation and Computer Vision'2008, Plzen, Czech Republic*, 2008, pp. 199–204.